Chapter 7
Synthesizing of Parallel Robots Using Adjusting Kinematic Parameters Method

P.R. Ouyang, W.J. Zhang, and J. Huang

Abstract Force balancing is a very important issue in mechanism design and has only recently been introduced to the design of robotic mechanisms. In this chapter, a force balancing method called adjusting kinematic parameters (AKP) for robotic mechanisms or real-time controllable (RTC) mechanisms is proposed, as opposed to existing force balancing methods, e.g., the counterweights (CW) method. Both the working principle of the AKP method and the design equation are described in detail. A particular implementation of the AKP method for the RTC mechanisms where two pivots on a link are adjustable is presented. After that, a hybrid approach to force balancing of robotic mechanisms is proposed, and this hybrid approach is to combine AKP and counterweights (CW) approaches, called AKP+CW in short. The main motivation of the AKP+CW approach is that CW and AKP each has its own advantage and disadvantage, and thus a combined one may strengthen both. This chapter presents the force balancing principles and equations for the AKP+CW approach. Software called ADAMS is employed as a tool for the simulated experiment to verify the effectiveness of the proposed approach. The joint forces and torques are calculated for the trajectory tracking of the RTC mechanisms. The implication of the work to the balancing of mechanisms in general is that many different force balancing methods may be combined based on the hybridization principle proposed in this chapter to become a novel one. Simulation results show that the AKP method and AKP+CW method are consistently better than the CW method in terms of the reduction of the joint forces and the torques in the servomotors, and the smoothing of the fluctuation of the joint force.

P.R. Ouyang (✉)
Department of Aerospace Engineering, Ryerson University, Toronto, ON, Canada
e-mail: pouyang@ryerson.ca

W.J. Zhang • J. Huang
Department of Mechanical Engineering, University of Saskatchewan, Saskatoon, SK, Canada

D. Zhang, B. Wei (eds.), *Dynamic Balancing of Mechanisms and Synthesizing of Parallel Robots*, DOI 10.1007/978-3-319-17683-3_7

7.1 Introduction

Mechanisms driven by real-time controllable (RTC) motors, or servomotors, are called RTC mechanisms. In general, RTC mechanisms are multi-degrees of freedom systems. RTC mechanisms are also called *mechatronic mechanisms*. A generic task of an RTC mechanism is to generate trajectory tracking motion. RTC mechanisms are fundamental building blocks in many machine tools and advanced robots due to their flexibility in terms of adapting to different applications without the need of redesign of their physical structures. Since there is no well-developed guidance available to design an RTC mechanism system with consideration of both control structures and mechanical structure designs, it is therefore significant to develop methodologies for this purpose.

For an RTC mechanism, the mechanical properties, such as shaking force balancing, shaking moment balancing, machine cooling, and vibration, are highly coupled with the characteristics of the controller. One challenging issue in the RTC mechanism design is that in order to achieve the optimal performance from the overall system viewpoint, both the controller design and the mechanical structure design need to be considered simultaneously. This chapter only takes the property of force balancing into consideration in addressing this issue. Force balancing can be categorized into static balancing problem and dynamic balancing problem. Static balancing is defined as a set of conditions under which the weight of the links of a mechanism does not produce any torque or force at the actuators under static conditions for any configuration of the manipulator or mechanism [1]. This is a mechanical solution which does not include solution by control method. This chapter focuses on static balancing. In this chapter, a parallel robot with two degrees of freedom is used as an example for the force balancing.

Many studies on force balancing of spatial mechanisms, i.e., robots, are performed at Laval University. These studies are limited within the scope of mechanical structure design only. When attached with a controller and programmed to follow different trajectories, however, mechanisms designed with complete force balancing property in this manner may not generate satisfactory dynamic performance. This consequence was revealed by the recent studies carried out at the Advanced Engineering Design Laboratory (AEDL) of the University of Saskatchewan [2] and other research [3].

At AEDL, a novel method called the adjusting kinematic parameters (AKP) method for force balancing of real-time controllable RTC mechanisms was developed [2]. This method suggests that adjusting the kinematic parameters can achieve force balancing of RTC mechanisms. Although showing advantages, there are some problems with this method. *First*, the initial development assumed that the center of mass of each link in a mechanism was in line with its axis; see Fig. 7.1a. However, in general, the center of mass of a link is likely off-line with its axis; see Fig. 7.1b. In mechanisms, a link may also take the ternary form instead of the binary form; see Fig. 7.1c. *Second*, the physical implementation was not considered in Wang's study. It should be noted that when adjusting the kinematic parameters of a link, extra

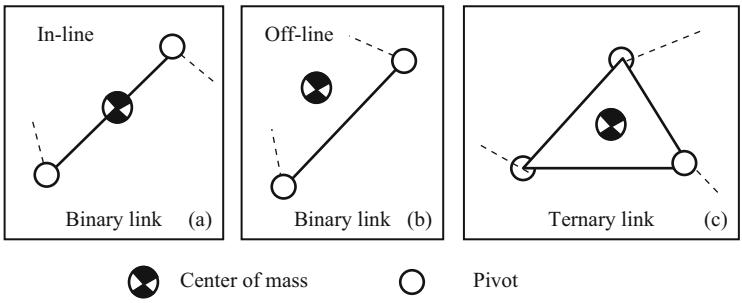

Fig. 7.1 Different situations of mass centers and different forms of links

masses are included in the system, and adjustment of kinematic parameters related to these masses may involve a change of the mass distribution of the system. *Third*, the exploration of how control methods affect trajectory tracking performance with respect to different force balancing methods was not well addressed. In particular, the control method used was a simple PD law with gains selected in a trial-and-error manner. *Finally*, trajectory planning was not well studied in spite of its importance in the AKP method. In fact, whenever the kinematic parameters are adjusted, the geometry of the mechanism may be varied; hence the trajectory must be re-planned to achieve the desired motion task.

7.2 Principles for Complete Force Balancing

There are two principles for complete force balancing: (1) making the total mass center of a mechanism stationary [4, 5], and (2) making the total potential energy of a mechanism stationary [1, 6]. *Principle* (1) is explained as follows.

Consider a mechanism that transmits forces to its base at point O. Let f_0 stand for the sum of the reacting forces the mechanism imposes on the base. The application of the Newton's second law leads to

$$\mathbf{f}_0 = -\frac{d}{dt}\{M\dot{\mathbf{r}}_c\} + M\mathbf{g} \tag{7.1}$$

where M is the total mass of a mechanism, $\mathbf{g}$ the gravitational acceleration, and $\dot{\mathrm{r}}_c$ the velocity of the *mass center* (MC) of the mechanism. It can be seen from Eq. (7.1) that the undesired shaking force results from changes in the system's linear momentum. This dynamic component becomes zero if the system MC does not change in any configuration, i.e., $\mathbf{r}_c = \mathbf{constant}$, during a period of motion. Therefore, *Principle (1)* can be stated as follows: to transmit zero shaking force, the mechanism's MC has to be stationary or configuration invariant. The property of configuration invariance of MC can be obtained in several ways, depending on the

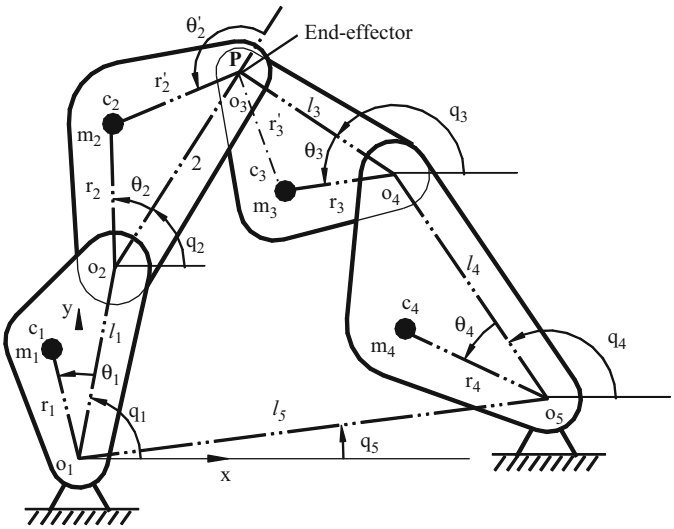

Fig. 7.2 A 2 DOF parallel robotic mechanism with arbitrary mass distribution

types of the mechanisms. For instance, for any mechanism containing only revolute kinematic pairs, the mass distribution of the mechanism to achieve the force balance can be obtained by using the *linearly independent vector* (LIV) approach [4].

The LIV approach is explained by taking a 2 DOF parallel robotic mechanism as an example; see Fig. 7.2. This mechanism consists of two kinematic chains connecting the fixed base and the end effector of the mechanism. The two kinematic chains are O_1, O_2, O_3, P and O_5, O_4, O_3, P, respectively. Two revolute actuators are mounted at joints O_1 and O_5 and described by joint variables q_1 and q_4, respectively. Joints O_2, O_3, and O_4 are passive revolute joints. Point P (overlapping with O_3) is the position of the end effector of the mechanism.

The stationary total mass center condition can be expressed by the following equation:

$$\mathbf{r}_c = \frac{1}{M}\sum_{i=1}^{4} m_i \mathbf{r}_i = \textbf{constant} \tag{7.2}$$

where m_i and $\mathbf{r}_i$ are the mass and the position vector of mass center of link i, respectively, and $M = \sum_{i=1}^{4} m_i$. According to the LIV approach, the position vector $\mathbf{r}_i$ in Eq. (7.2) can be expressed as

$$\begin{cases} \mathbf{r}_1 = r_1 \mathrm{e}^{\mathbf{i}(q_1+\theta_1)} \\ \mathbf{r}_2 = l_1 \mathrm{e}^{\mathbf{i}q_1} + r_2 \mathrm{e}^{\mathbf{i}(q_2+\theta_2)} \\ \mathbf{r}_3 = l_5 \mathrm{e}^{\mathbf{i}q_5} + l_4 \mathrm{e}^{\mathbf{i}q_4} + r_3 \mathrm{e}^{\mathbf{i}(q_3+\theta_3)} \\ \mathbf{r}_4 = l_5 \mathrm{e}^{\mathbf{i}q_5} + r_4 \mathrm{e}^{\mathbf{i}(q_4+\theta_4)} \end{cases} \tag{7.3}$$

Substituting Eq. (7.3) into Eq. (7.2) leads to

$$\begin{aligned} M\mathbf{r}_c = {} & \left(m_3 l_5 \mathrm{e}^{\mathbf{i}q_5} + m_4 l_5 \mathrm{e}^{\mathbf{i}q_5}\right) + \left(m_1 r_1 \mathrm{e}^{\mathbf{i}\theta_1} + m_2 l_1\right) \mathrm{e}^{\mathbf{i}q_1} + \left(m_2 r_2 \mathrm{e}^{\mathbf{i}\theta_2}\right) \mathrm{e}^{\mathbf{i}q_2} \\ & + \left(m_3 r_3 \mathrm{e}^{\mathbf{i}\theta_3}\right) \mathrm{e}^{\mathbf{i}q_3} + \left(m_4 r_4 \mathrm{e}^{\mathbf{i}\theta_4} + m_3 l_4\right) \mathrm{e}^{\mathbf{i}q_4} \end{aligned} \tag{7.4}$$

The unit vectors $\mathrm{e}^{\mathbf{i}q_1}$, $\mathrm{e}^{\mathbf{i}q_2}$, $\mathrm{e}^{\mathbf{i}q_3}$, and $\mathrm{e}^{\mathbf{i}q_4}$ are constrained by the kinematic closed-loop equation, i.e., $l_1 \mathrm{e}^{\mathbf{i}q_1} + l_2 \mathrm{e}^{\mathbf{i}q_2} - l_3 \mathrm{e}^{\mathbf{i}q_3} - l_4 \mathrm{e}^{\mathbf{i}q_4} - l_5 \mathrm{e}^{\mathbf{i}q_5} = 0$. Substituting this constraint equation into Eq. (7.4) leads to

$$\begin{aligned} M\mathbf{r}_c = {} & \left(m_3 l_5 \mathrm{e}^{\mathbf{i}q_5} + m_4 l_5 \mathrm{e}^{\mathbf{i}q_5} + \lambda_{25} m_2 r_2 \mathrm{e}^{\mathbf{i}\theta_2} \mathrm{e}^{\mathbf{i}q_5}\right) \\ & + \left(m_1 r_1 \mathrm{e}^{\mathbf{i}\theta_1} + m_2 l_1 - \lambda_{21} m_2 r_2 \mathrm{e}^{\mathbf{i}\theta_2}\right) \mathrm{e}^{\mathbf{i}q_1} + \left(m_3 r_3 \mathrm{e}^{\mathbf{i}\theta_3} + \lambda_{23} m_2 r_2 \mathrm{e}^{\mathbf{i}\theta_2}\right) \mathrm{e}^{\mathbf{i}q_3} \\ & + \left(m_4 r_4 \mathrm{e}^{\mathbf{i}\theta_4} + m_3 l_4 + \lambda_{24} m_2 r_2 \mathrm{e}^{\mathbf{i}\theta_2}\right) \mathrm{e}^{\mathbf{i}q_4} \end{aligned} \tag{7.5}$$

where $\lambda_{ij} = {}^{l_j}\!/_{l_i}$, $i, j = 1, \ldots, 5$. In order to make the total mass center stationary, all the terms with the time-varying quantities (q_1, q_3 and q_4) in Eq. (7.5) should vanish. This will result in the following equations:

$$m_1 r_1 \mathrm{e}^{\mathbf{i}\theta_1} + m_2 l_1 - \lambda_{21} m_2 r_2 \mathrm{e}^{\mathbf{i}\theta_2} = 0 \tag{7.6}$$

$$m_3 r_3 \mathrm{e}^{\mathbf{i}\theta_3} + \lambda_{23} m_2 r_2 \mathrm{e}^{\mathbf{i}\theta_2} = 0 \tag{7.7}$$

$$m_4 r_4 \mathrm{e}^{\mathbf{i}\theta_4} + m_3 l_4 + \lambda_{24} m_2 r_2 \mathrm{e}^{\mathbf{i}\theta_2} = 0 \tag{7.8}$$

As long as Eqs. (7.6) to (7.8) are satisfied in the design process, the shaking force of the parallel robotic mechanism is cancelled. Such a mechanism is called a force balanced mechanism.

Principle (2) is that if the total potential energy of a mechanism in any configuration is kept constant (i.e., the weight of the mechanism has no effect on the actuators), then the mechanism is force balanced. The expression of the total potential energy of the mechanism can be written as

$$V = V_w + V_s \tag{7.9}$$

where V_w and V_s are, respectively, the gravitational potential energy and the elastic potential energy stored in the springs. The way of implementing this principle is to eliminate the effect of the potential energy through properly adding springs into the original mechanism [1].

As shown in Fig. 7.1, two relationships $r_2 e^{i\theta_2} = l_2 + r'_2 e^{i\theta'_2}$ and $r_3 e^{i\theta_3} = l_3 + r'_3 e^{i\theta'_3}$ can be readily obtained. By using these relationships, Eqs. (7.6)–(7.8) can be rewritten as

$$m_1 r_1 l_2 = l_1 m_2 r'_2 \quad \text{and} \quad \theta_1 = \theta'_2 \tag{7.10}$$

$$m_3 r_3 l_2 = l_3 m_2 r_2 \quad \text{and} \quad \theta_3 = \pi + \theta_2 \tag{7.11}$$

$$m_4 r_4 l_3 = l_4 m_3 r'_3 \quad \text{and} \quad \theta_4 = \theta'_3 \tag{7.12}$$

From the above three equations, it can be seen that whenever the mass distribution of one of the links is given, the mass distributions of the remaining three links can be determined. The equations to calculate the additional masses can be derived as (assume that link 2 is unchanged)

$$m_i^* r_i^* e^{i\theta_i^*} = m_i r_i e^{i\theta_1} - m_i^0 r_i^0 e^{i\theta_i^0} \quad (i = 1, 3, 4) \tag{7.13}$$

where m_i^0, r_i^0, and θ_i^0 are the parameters of the original link; m_i^*, r_i^*, and θ_i^* are the parameters of the counterweights (CW); and m_i, r_i, and θ_i are the parameters after adding or deducting the counterweights to the original mechanism.

Apparently, in general, either m_i^* or r_i^* is arbitrarily selected, then the other one can be obtained from Eq. (7.13).

There are several problems associated with the CW method. The first problem is that both joint forces and actuator output torques might increase. The second problem is that the vibration behavior of the mechanism may be degraded [3]. The third problem is that the balanced mechanism may have a poor trajectory tracking performance, and consume more energy when running at high speeds [7, 8]. Although a careful design of the mass redistribution may help in solving these problems to some degree, new methods are needed for further improvement. It should be further noted that the CW method is only applicable to pivot joint mechanisms.

7.3 New Force Balancing Condition Equations

When implementing the extended AKP method, the masses of sliding blocks, which are used to adjust the pivots, must be taken into account in the force balancing condition equations. The implementation of the pivot adjustment is illustrated in Fig. 7.3 [7, 8]. When sliding block 3 is adjusted along link 1 or sliding block 4 adjusted along link 2, the mass distribution of this group of links will vary.

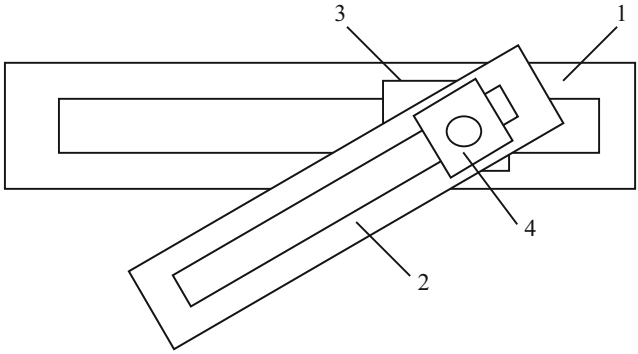

Fig. 7.3 Illustration of pivot adjustment

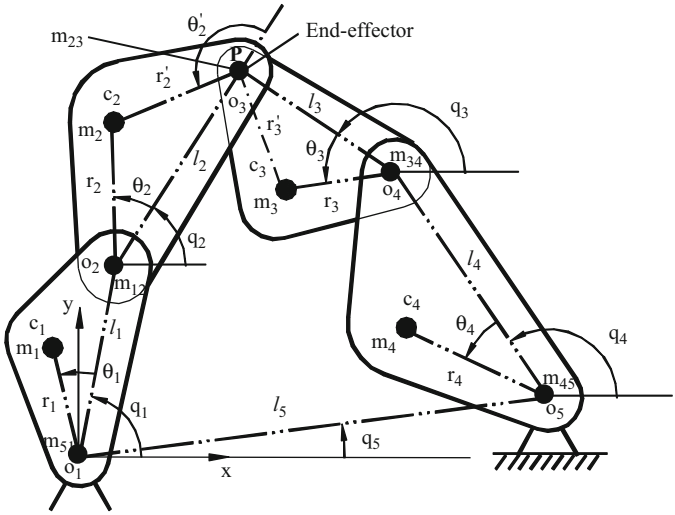

Fig. 7.4 Scheme of parallel robotic mechanism with the point mass at the pivot

Assume that the sliding block is a point mass acting on the pivot, denoting m_{ij} as the mass of the sliding block between link i and link j. The schematic diagram of the parallel robotic mechanism with consideration of these point masses, m_{ij}, is shown in Fig. 7.4.

The new force balancing condition equations can be derived by following the LIV approach:

$$m_1 r_1 \mathrm{e}^{i\theta_1} + (m_2 + m_{12})\, l_1 - l_1 m_2 r_2 \mathrm{e}^{i\theta_2}/l_2 = 0 \tag{7.14}$$

$$m_3 r_3 \mathrm{e}^{i\theta_3} + m_{23} l_3 + l_3 m_2 r_2 \mathrm{e}^{i\theta_2}/l_2 = 0 \tag{7.15}$$

$$m_4 r_4 e^{i\theta_4} + (m_3 + m_{23} + m_{34}) l_4 + l_4 m_2 r_2 e^{i\theta_2}/l_2 = 0 \tag{7.16}$$

Using the relationship $r_2 e^{\mathbf{i}\theta_2} = l_2 + r_2' e^{\mathbf{i}\theta_2'}$, Eq. (7.14) can be rewritten as

$$l_2 m_1 r_1 e^{i\theta_1} = l_1 m_2 \tilde{r}_2' e^{i\tilde{\theta}_2'} \tag{7.17}$$

where $\tilde{r}_2' = \sqrt{\left(r_2' \cos\theta_2' - m_{12} l_2/m_2\right)^2 + \left(r_2' \sin\theta_2'\right)^2}$

$$\tilde{\theta}_2' = \tan^{-1}\left(\frac{r_2' \sin\theta_2'}{r_2' \cos\theta_2' - m_{12} l_2/m_2}\right)$$

Similarly, Eq. (7.15) can be rewritten as

$$l_2 m_3 r_3 e^{i\theta_3} + l_3 m_2 \tilde{r}_2 e^{i\tilde{\theta}_2} = 0 \tag{7.18}$$

where $\tilde{r}_2 = \sqrt{(r_2 \cos\theta_2 + m_{23} l_2/m_2)^2 + (r_2 \sin\theta_2)^2}$

$$\tilde{\theta}_2 = \tan^{-1}\left(\frac{r_2 \sin\theta_2}{r_2 \cos\theta_2 + m_{23} l_2/m_2}\right)$$

Likewise, Eq. (7.16) can be rewritten as

$$l_2 m_4 r_4 e^{i\theta_4} + l_4 m_2 \widehat{r}_2 e^{i\widehat{\theta}_2} = 0 \tag{7.19}$$

where $\widehat{r}_2 = \sqrt{(r_2 \cos\theta_2 + (m_3 + m_{23} + m_{34}) l_2/m_2)^2 + (r_2 \sin\theta_2)^2}$

$$\widehat{\theta}_2 = \tan^{-1}\left(\frac{r_2 \sin\theta_2}{r_2 \cos\theta_2 + (m_3 + m_{23} + m_{34}) l_2/m_2}\right)$$

Eqs. (7.17) to (7.19) are the new force balancing equations and can be rearranged as

$$l_2 m_1 r_1 = l_1 m_2 \tilde{r}_2' \quad \text{and} \quad \theta_1 = \tilde{\theta}_2' \tag{7.20}$$

$$l_2 m_3 r_3 = l_3 m_2 \tilde{r}_2 \quad \text{and} \quad \theta_3 = \tilde{\theta}_2 + \pi \tag{7.21}$$

$$l_2 m_4 r_4 = l_4 m_2 \widehat{r}_2 \quad \text{and} \quad \theta_4 = \widehat{\theta}_2 + \pi \tag{7.22}$$

Compared with the original force balancing Eqs. (7.10)–(7.12), it can be seen that the effect due to the sliding blocks is reflected by the augmented parameters, i.e., $(\tilde{r}_2, \tilde{r}_2', \widehat{r}_2)$ and $(\tilde{\theta}_2, \tilde{\theta}_2', \widehat{\theta}_2)$, which are only related to link 2, the masses of the sliding

blocks, and link 3. The force balancing condition equations, i.e., Eqs. (7.20)–(7.22), imply that the mass distribution of a force balanced mechanism should satisfy Eqs. (7.20)–(7.22). It is noted that the force balancing condition equations above are derived by following principle (1), and therefore, they are applicable to the AKP method.

7.4 The Extended AKP Method

Examining the original and the new force balancing equations shown in Eqs. (7.10) to (7.12) and Eqs. (7.20) to (7.22), respectively, it is clear that these equations can also be satisfied by changing the kinematic parameters, l_i ($i = 1, 2, 3, 4$), whilst maintaining the total mass of a mechanism unchanged. It should be noted that when l_i is varied, the parameters r_i and θ_i will be changed accordingly. Both the original and the extended AKP method are developed based on this observation. In particular, the derivation of the extended AKP method based on the new force balancing equations is given as follows [9]. A general design case will be presented first, followed by a special design case.

In the general design situation, assume that the mass centers of the links are arbitrarily distributed, with $\theta_i \neq 0$ for $i = 1$ to 4, as shown in Fig. 7.5. Let l_i^0 and (r_i^0, θ_i^0) represent the length and the mass center of link i, respectively, where superscript "0" indicates the parameters prior to the adjustment of pivot o_i^0. It is observed that in order to satisfy the force balancing condition equations specified in Eqs. (7.20) to (7.22), adjusting of only one pivot on a link is not sufficient; instead, two pivots must be adjusted. The extended AKP method is thus accomplished in two steps. The first step is to adjust a pivot from o_i^0 to o_i so that the angle relationship between link i and link $i + 1$ can be satisfied. The second step is to adjust o_{i+1}^0 to o_{i+1} so that all Eqs. (7.20) to (7.22) can be satisfied. Now, let l_i and (r_i, θ_i) represent the new length and the new mass center of link i, respectively, and let v_i and w_i represent the adjusted amounts of the two pivots o_i and o_{i+1}, respectively. From Fig. 7.5, the following equations can be obtained:

$$l_i = l_i^0 - v_i - w_i \tag{7.23}$$

$$r_i^0 \cos\theta_i^0 = v_i + r_i \cos\theta_i \tag{7.24}$$

$$r_i^0 \sin\theta_i^0 = r_i \sin\theta_i \tag{7.25}$$

for $i = 1, 2, 3, 4$.

Equation (7.25) can be rewritten as

$$r_i = \frac{r_i^0 \sin\theta_i^0}{\sin\theta_i} \tag{7.26}$$

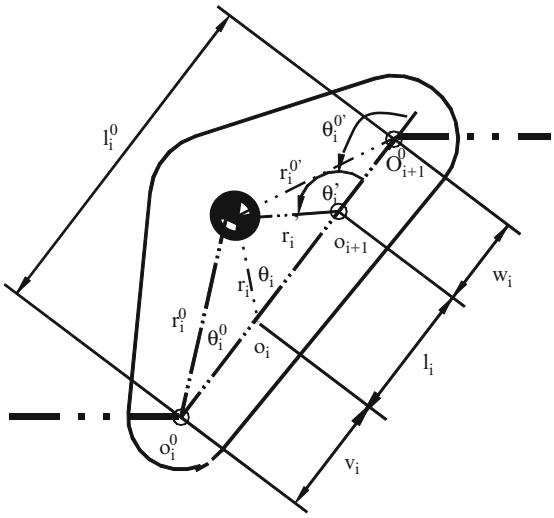

Fig. 7.5 Two-step kinematic parameter adjustment in the extended AKP method

Substituting Eq. (7.26) into Eq. (7.24) yields

$$v_i = r_i^0 \sin\left(\theta_i - \theta_i^0\right) / \sin\theta_i \tag{7.27}$$

Based on the force balancing condition equations given in Eqs. (7.20) to (7.22) and the results given in Eqs. (7.23) to (7.27), the implementation of the extended AKP method can be illustrated using the following example. Referring to Fig. 7.4, assume that the pivots of link 2 are unchanged, and the force balancing conditions can be achieved by adjusting the pivots of the other three links. The detailed procedure is illustrated below.

For link 1:

Pivot O_1 on link 1 is adjusted using the following equation derived from Eqs. (7.27) and (7.20):

$$v_1 = r_1^0 \sin\left(\tilde{\theta}_2' - \theta_1^0\right) / \sin\tilde{\theta}_2' \tag{7.28}$$

Pivot O_2 on link 1 is adjusted using Eq. (7.20). To determine the amount of adjustment for pivot O_2 on link 1, i.e., w_1, substituting Eq. (7.28) and Eqs. (7.23) to (7.25) into Eq. (7.20) yields

$$w_1 = l_1^0 - \frac{r_1^0\left(m_2\tilde{r}_2' \sin\left(\tilde{\theta}_2' - \theta_1^0\right) + m_1 l_2 \sin\theta_1^0\right)}{m_2\tilde{r}_2' \sin\tilde{\theta}_2'} \tag{7.29}$$

For link 3:
Substituting Eq. (7.21) into Eq. (7.27) yields

$$v_3 = r_3^0 \sin\left(\tilde{\theta}_2 - \theta_3^0\right) / \sin\tilde{\theta}_2 \tag{7.30}$$

Substituting Eq. (7.30) and Eqs. (7.23) to (7.25) into Eq. (7.21) yields

$$w_3 = l_3^0 - \frac{r_3^0\left(m_2\tilde{r}_2 \sin\left(\tilde{\theta}_2 - \theta_3^0\right) - m_3 l_2 \sin\theta_3^0\right)}{m_2\tilde{r}_2 \sin\tilde{\theta}_2} \tag{7.31}$$

For link 4:
Substituting Eq. (7.22) into Eq. (7.27) yields

$$v_4 = r_4^0 \sin\left(\widehat{\theta}_2 - \theta_4^0\right) / \sin\widehat{\theta}_2 \tag{7.32}$$

Substituting Eq. (7.32) and Eqs. (7.23) to (7.25) into Eq. (7.22) yields

$$w_4 = l_4^0 - \frac{r_4^0\left(m_2\widehat{r}_2 \sin\left(\widehat{\theta}_2 - \theta_4^0\right) - m_4 l_2 \sin\theta_4^0\right)}{m_2\widehat{r}_2 \sin\widehat{\theta}_2} \tag{7.33}$$

For the special design case where mass distributions of all the links are in line with their kinematic axes, adjusting of only one pivot for each link is sufficient. In this case, since conditions $\theta_i^0 = 0$ and $\theta_i = 0$ hold, Eq. (7.25) thus becomes meaningless. Furthermore, if the sliding blocks are not considered in the implementation, the force balancing equations given in Eqs. (7.23) to (7.25) are simplified as the original ones given in Eqs. (7.10) to (7.12). Substituting Eqs. (7.23) and (7.24) into Eqs. (7.10) to (7.12), the adjusting amounts for links 1, 3, and 4, respectively, can be obtained as follows:

$$v_1 = \left(m_2 r_2' l_1^0 \cos\theta_1 - m_1 r_1^0 l_2 \cos\theta_1^0\right) / \left(m_2 r_2' \cos\theta_1 - m_1 l_2\right) \tag{7.34}$$

$$v_3 = \left(m_2 r_2 l_3^0 \cos\theta_3 - m_3 r_3^0 l_2 \cos\theta_3^0\right) / \left(m_2 r_2 \cos\theta_3 - m_3 l_2\right) \tag{7.35}$$

$$v_4 = \left(k l_4^0 \cos\theta_4 - m_4 r_4^0 \cos\theta_4^0\right) / \left(k \cos\theta_4 - m_4\right) \tag{7.36}$$

with $k = \sqrt{(m_2 r_2 / l_2)^2 + m_3^2 + (2 m_2 r_2 m_3 \cos\theta_2 / l_2)}$.

Moreover, following the above discussion, if link 3 is selected to be unchanged, the adjusting amounts for other three links can be determined as follows:

$$v_1 = \left(h l_1^0 \cos\theta_1 - m_1 r_1^0 \cos\theta_1^0\right) / \left(h \cos\theta_1 - m_1\right) \tag{7.37}$$

$$v_2 = \left(m_3 r_3 l_2^0 \cos\theta_2 - m_2 r_2^0 l_3 \cos\theta_2^0\right) / \left(m_3 r_3 \cos\theta_2 - m_2 l_3\right) \tag{7.38}$$

$$v_4 = \left(m_3 r_3' l_4^0 \cos\theta_4 - m_4 r_4^0 l_3 \cos\theta_4^0\right) / \left(m_3 r_3' \cos\theta_4 - m_4 l_3\right) \tag{7.39}$$

with $h = \sqrt{(m_3 r_3/l_3)^2 + m_2^2 + (2 m_3 r_3 m_2 \cos\theta_3/l_3)}$.

When designing an RTC mechanism, for a given task, i.e., a set of trajectory points that the end effector should follow, through the inverse kinematics, the corresponding joint angles are readily determined. However, if the extended AKP method is adopted for force balancing design, the kinematic parameters of the mechanism will vary. This will in turn change the inverse kinematics of the mechanism. In order to enable the end effector of the mechanism to follow the same trajectory, the motion profiles of the joints must be adjusted according to the new inverse kinematics. This adjustment is only possible through the implementation of programmable actuators, i.e., RTC actuators. Therefore, the application of the extended AKP method is only limited to RTC mechanisms.

To verify the extended AKP method, a parallel robotic mechanism prototype was built using LEGO blocks, as shown in Fig. 7.6. Figure 7.6a shows the unbalanced system. After applying the extended AKP method, the kinematic parameters were changed and the shaking force of the mechanism was cancelled. Figure 7.6b, c illustrates two configurations of the force balanced mechanism. The mechanism was stabilized at these two positions, and in fact, it was stable at any other positions as well. That is, the mechanism is force balanced.

7.5 Comparison of the Extended AKP Method with the CW Method: Joint Reaction Force

Two examples are used here to verify the effectiveness of the extended AKP method. Comparison is made between the extended AKP method and the CW method in terms of reduction of the joint forces.

Example 1 The kinematic parameters of the original mechanism without considering force balancing are listed in Table 7.1. Using the CW method and the extended AKP method, the kinematic parameters of the force balanced mechanism are computed and listed in the same table. In the CW case, assume that link 3 is unchanged and the other three links are subject to additional masses. In the extended AKP case, assume that all the movable links are subject to pivot adjustments.

The mechanism is supposed to fulfill the following task: the end effector is requested to move from point A (0.3, 0.2) to point B (0.2, 0.3) within 1 s, and subsequently to point C (0.1, 0.2) within 2 s. The unit of the coordinates is meter for all examples. Furthermore, for each segment of the trajectories, (1) the velocities of the end effector at these three points are zero, and (2) the accelerations of the end

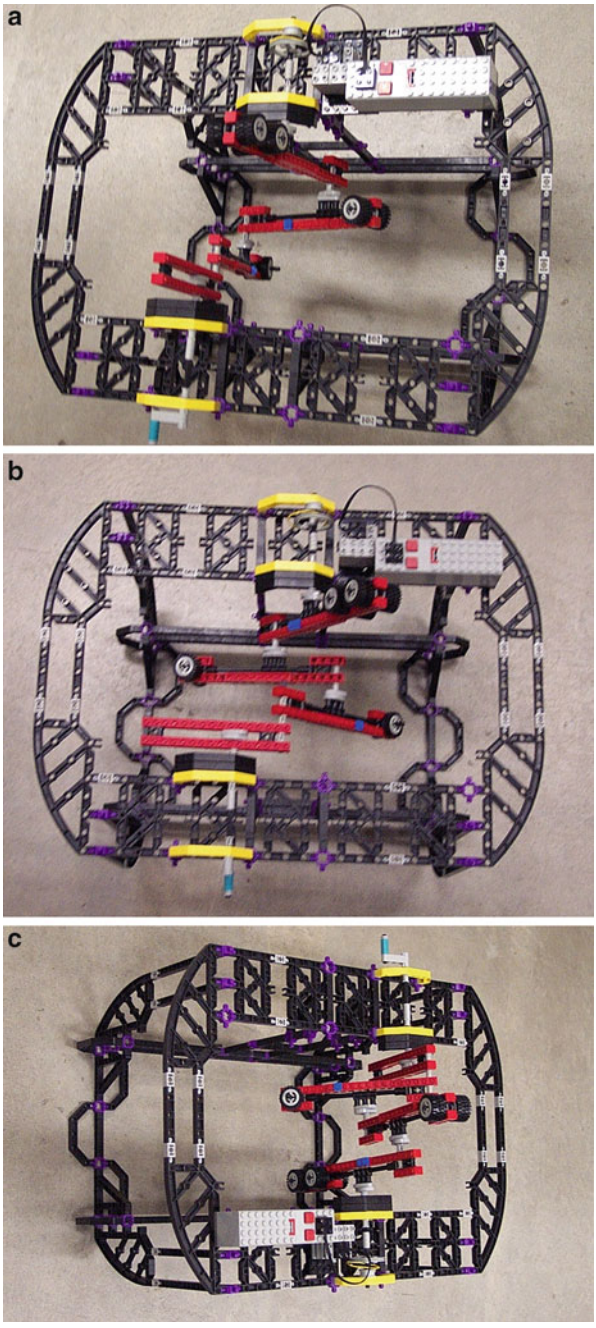

Fig. 7.6 (**a**) Unbalanced mechanism. (**b**) Balanced mechanism using the extended AKP method (1). (**c**) Balanced mechanism using the extended AKP method (2)

Table 7.1 Parameters for different mechanisms (in-line case 1)

Parameters	Unbalanced linkage	CW linkage	AKP linkage
l_1 (m)	0.2	0.2	0.0977
l_2 (m)	0.3	0.3	0.28
l_3 (m)	0.4	0.4	0.2445
l_4 (m)	0.3	0.3	0.1009
l_5 (m)	0.3	0.3	0.3
r_1 (m)	0.05	0.1758	0.0523
r_2 (m)	0.15	0.0506	0.13
r_3 (m)	0.08	0.08	0.0756
r_4 (m)	0.1	0.103	0.0991
m_1 (kg)	0.25	0.5912	0.25
m_2 (kg)	0.25	0.4445	0.25
m_3 (kg)	0.375	0.375	0.375
m_4 (kg)	0.5	0.8742	0.5
I_1 $(\text{kg} \cdot \text{m}^2)$	0.004	0.0133	0.004
I_2 $(\text{kg} \cdot \text{m}^2)$	0.01	0.0229	0.01
I_3 $(\text{kg} \cdot \text{m}^2)$	0.02	0.02	0.02
I_4 $(\text{kg} \cdot \text{m}^2)$	0.02	0.0475	0.02
θ_1(rad)	0	π	π
θ_2(rad)	0	π	0
θ_3(rad)	0	0	π
θ_4(rad)	0	π	π

effector at the initial and final points are zero. The trajectories at the two actuators can be determined based on the inverse kinematic and the motion planning method that will be described in Chap. 4. In particular, the trajectories at the two actuators for the unbalanced mechanism and the force balanced mechanism using the CW method are, respectively, expressed as follows:

For actuator 1:

$$q_1(t) = 90.0 + 187.2701 \times t^3 - 261.4406 \times t^4 + 96.7905 \times t^5 \quad \text{if } t \leq 1$$

$$q_1(t) = 112.6199 - 38.9289 \times (t-1)^2 + 109.4122 \times (t-1)^3 - 67.4608 \times (t-1)^4 + 12.5189 \times (t-1)^5 \quad \text{if} \quad 1 < t \leq 3$$

For actuator 2:

$$q_4(t) = -13.688 + 657.9647 \times t^3 - 894.1248 \times t^4 + 320.5211 \times t^5 \quad \text{if } t \leq 1$$

$$q_4(t) = 27.5324 - 87.5649 \times (t-1)^2 + 157.4044 \times (t-1)^3 - 85.2165 \times (t-1)^4 + 14.8542 \times (t-1)^5 \quad \text{if} \quad 1 < t \leq 3$$

As mentioned in Sect. 4, the trajectory of the force balanced mechanism using the extended AKP method must be re-planned due to the change of the kinematic parameters. After re-planning, the expressions of the new trajectories at the two actuators are as follows:

For actuator 1:

$$q_1(t) = 63.4541 + 201.7492 \times t^3 - 290.3993 \times t^4 + 111.27 \times t^5 \quad \text{if } t \leq 1$$

$$q_1(t) = 86.0739 - 24.4488 \times (t-1)^2 + 152.8515 \times (t-1)^3 - 105.4703 \times (t-1)^4 + 20.4828 \times (t-1)^5 \quad \text{if} \quad 1 < t \leq 3$$

For actuator 2:

$$q_4(t) = -13.688 + 657.9647 \times t^3 - 894.1248 \times t^4 + 320.5211 \times t^5 \qquad \text{if } t \leq 1$$

$$q_4(t) = 70.6729 - 185.6443 \times (t-1)^2 + 286.676 \times (t-1)^3 - 145.3904 \times (t-1)^4 + 24.437 \times (t-1)^5 \quad \text{if} \quad 1 < t \leq 3$$

Using the software called "Working Model 2D" (Knowledge Revolution, 1999), the joint forces in the five pivots can be calculated. Figure 7.7 shows the joint forces in the two actuators.

It can be seen from Fig. 7.7 that, when the mechanism runs at low speeds (about 5 rpm), the forces in the two actuators for the force balanced mechanism do not change very much, and the extended AKP method insures smaller forces at both the x-direction and the y-direction than the CW method. Furthermore, the joint forces at the y-direction using the CW method are significantly larger than those of the extended AKP method and the unbalanced mechanism. This phenomenon agrees with one of the weaknesses associated with the CW method; that is, joint forces will be increased. It is interesting to observe that the variations of joint forces using both the CW and the extended AKP methods are small, while the joint forces of the unbalanced mechanism vary considerably, especially in the x-direction. The reason for this phenomenon can be explained as follows. After the shaking force is balanced, the mass center of the system is stationary during operation. Furthermore, the inertia term is small at low speeds. Therefore, the variation of the forces in the two actuators is small. On the other hand, for the unbalanced mechanism, the mass center of the mechanism changes with the system configurations. Therefore, variation of the forces in the two actuators is large.

It should be noted that, for the force balanced mechanism, the total forces at the two actuators should be zero in the x-direction and should be equal to the total weight of the mechanism in the y-direction. This observation is confirmed with the results shown in Fig. 7.7.

Figure 7.8 shows the results when the mechanism runs at high speeds (about 50 rpm). Performance totally different from the low-speed motion is observed.

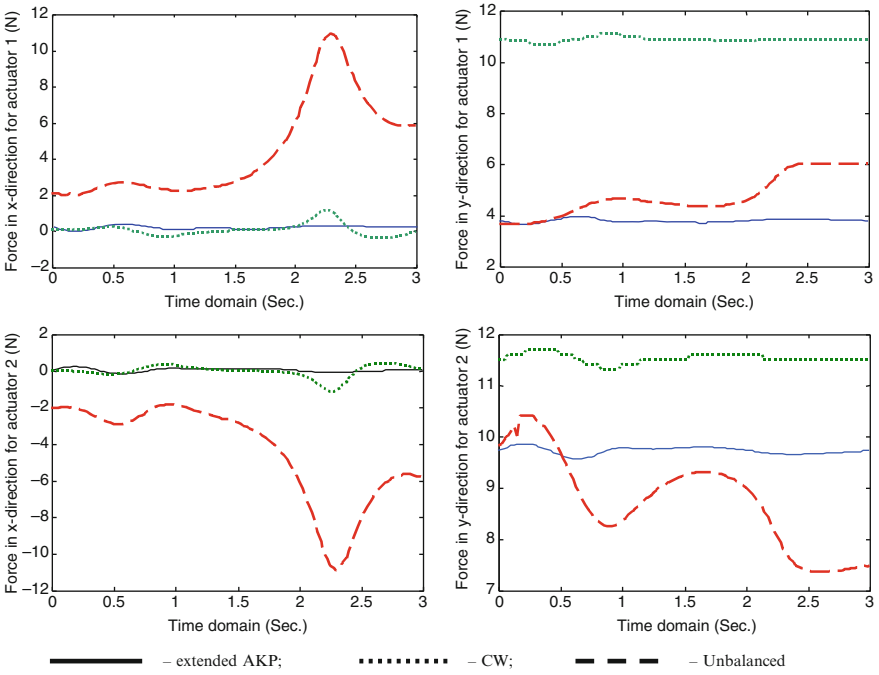

Fig. 7.7 Joint forces in the two actuators at low speeds

First, variations of the forces are very large for all three cases. Second, the CW method generates the worst performance in the x-direction; although the total forces in the two actuators in the x-direction are still maintained at zero, the sharp variation of forces exhibits. Nevertheless, the extended AKP method remains to produce the best performance.

The results above are expected. When the mechanism runs at high speeds, the inertia forces becomes the dominant term in the dynamics. Since the CW method adopts the adding mass approach for force balancing purpose, its inertia force takes more weight. While with the extended AKP method, the total mass of the system is unchanged; therefore the inertia force does not differ significantly from the unbalanced mechanism.

To further illustrate the effectiveness of the extended AKP method, Table 7.2 lists the minimum and maximum joint forces in the x-direction and the y-direction for the cases of applying the AKP method and the CW method, respectively. It is observed that the joint forces generated by using the extended AKP method have a smaller variation range than those using the CW method. The reduction of the forces in the x-direction is more remarkable by using the AKP method than by using the CW method.

Example 2 In this example, a mechanism with the mass center off-line of the kinematic axis is studied. The kinematic parameters of the original mechanism

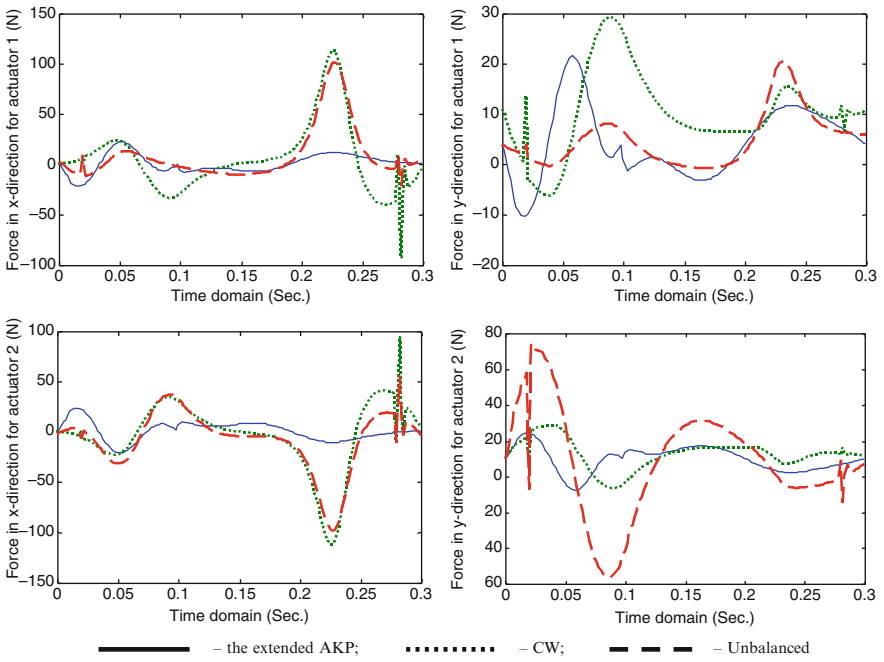

Fig. 7.8 Joint forces in the two actuators at high speeds

Table 7.2 Joint forces (min and max) using different force balancing methods

		Joint forces in *x*-direction				Joint forces in *y*-direction			
		AKP method		CW method		AKP method		CW method	
Speeds	Pivot no.	Min	Max	Min	Max	Min	Max	Min	Max
Low speeds	1	−0.205	0.204	−0.405	1.130	3.640	3.930	10.70	11.10
	2	−0.208	0.228	−1.210	0.338	−1.470	−1.200	−5.350	−4.870
	3	−0.233	0.164	−1.130	0.387	0.930	1.320	−0.869	−0.595
	4	−0.514	0.444	−1.140	0.487	4.320	5.300	2.430	3.420
	5	−0.204	0.205	−1.130	0.405	9.560	9.840	11.30	11.70
High speeds	1	−22.80	21.60	−93.50	113.0	−10.50	21.40	−6.40	29.20
	2	−21.30	25.00	−121.0	81.00	−18.10	11.80	−31.10	17.30
	3	−24.20	18.30	−113.0	89.40	−21.90	22.30	−14.10	13.30
	4	−56.90	42.10	−114.0	110.0	−50.10	60.70	−48.30	51.90
	5	−21.60	22.80	−113.0	93.50	−7.870	23.90	−6.770	28.80

without force balancing and the modified mechanisms using the CW method and the extended AKP method are listed in Table 7.3, respectively. In the redesign of the mechanism, link 2 is assumed to be unchanged.

In this example, the mechanism is supposed to fulfill the following task: the end effector is requested to move from point A (0.3, 0.25) to point C (0.1, 0.2)

Table 7.3 Parameters for different mechanisms (off-line)

Parameters	Unbalanced linkage	CW linkage	AKP linkage
l_1 (m)	0.15	0.15	0.0866
l_2 (m)	0.26	0.26	0.26
l_3 (m)	0.26	0.26	0.2078
l_4 (m)	0.14	0.14	0.08838
l_5 (m)	0.30	0.30	0.30
r_1 (m)	0.075	0.0866	0.10
r_2 (m)	0.15	0.15	0.15
r_3 (m)	0.08485	0.10	0.12
r_4 (m)	0.115	0.1415	0.135
m_1 (kg)	1	2	1
m_2 (kg)	2	2	2
m_3 (kg)	2	3	2
m_4 (kg)	2	4	2
I_1 $(\text{kg} \cdot \text{m}^2)$	0.01	0.03	0.01
I_2 $(\text{kg} \cdot \text{m}^2)$	0.05	0.05	0.05
I_3 $(\text{kg} \cdot \text{m}^2)$	0.04	0.06	0.04
I_4 $(\text{kg} \cdot \text{m}^2)$	0.02	0.04	0.02
θ_1(deg)	90	150	150
θ_2(deg)	30	30	30
θ_3(deg)	225	210	210
θ_4(deg)	192.83	169.11	188.21

and intermediate point B (0.2, 0.2). The time duration between two neighboring points is 2 s at low speeds (about 5 rpm) and 0.1 s at high speeds (about 100 rpm). Furthermore, for each segment of the trajectories, (1) the velocity of the end effector at the intermediate point B is determined by the method that will be discussed in Chap. 4, and (2) the accelerations of the end effector at the initial and final tracking points are zero.

Figures 7.9 and 7.10 show the total forces in the two actuators for the unbalanced mechanism and the balanced mechanism using the extended AKP method and the CW method at low speeds and high speeds, respectively. From these two figures, it can be seen that the extended AKP method is the best in terms of the reduction of forces at both low speeds and high speeds, and the CW method is the worst. So it is demonstrated that the extended AKP method is better than the CW method in the reduction of the joint forces for an off-line mechanism.

From the force profiles shown in these figures, it can be seen that, in order to accomplish the same motion task, the extended AKP method needs the least amount of forces at both low speeds and high speeds among all the three design cases. The CW method, however, demands the highest forces. The extended AKP method is thus demonstrated to be better than the CW method in terms of the joint force reductions.

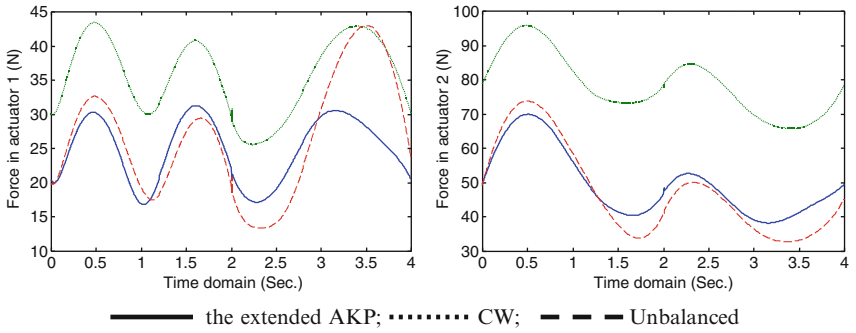

Fig. 7.9 Total forces in the two actuators at low speeds

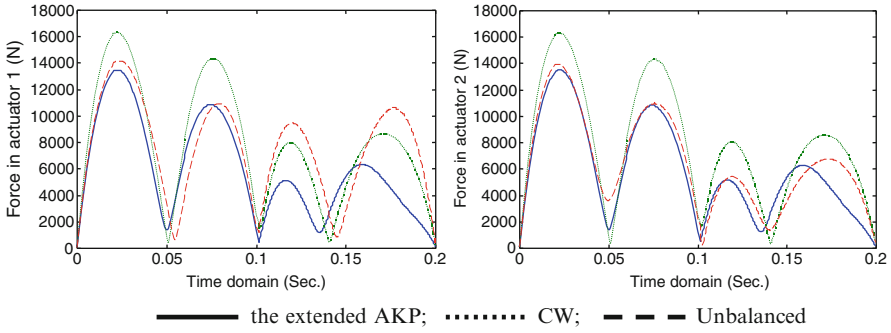

Fig. 7.10 Total forces in the two actuators at high speeds

However, the adjustment of the kinematic parameters may not always work in some applications. One case of the failure with the AKP approach is such that the trajectory may be out of the new workspace which results from the change of the kinematic parameters of the mechanism [9]. The other case is that a required change in the kinematics parameter may be out of the physical region. Another shortcoming with AKP is an increase in complexity of the mechanism structure. In the next section, a new solution will be introduced, that is, the hybridization of AKP and CW method.

7.6 Hybrid AKP+CW Method for Force Balancing

To overcome the limitations of both the CW method and the AKP method, we propose a force balancing strategy which combines these two methods in the pursuit of taking advantages of both the methods while alleviating their shortcomings. The generalized one of this strategy is called "hybridization engineering" [10]. Through such a hybrid approach, it is possible that a good performance and a

limited workspace modification of the designed RTC mechanism can be achieved. The same configuration shown in Fig. 7.4 will be considered as an example for the implementation of the hybrid AKP+CW method [11].

7.6.1 Hybrid AKP+CW Method

In the following discussion, we also consider that link 2 in Fig. 7.4 is unchanged without the loss of generality. We use the following notation for the particular schemes of the CW+AKP method: "1CW+3/4AKP" means CW is applied to link 1, and AKP is applied to link 3 and link 4, respectively. We consider two particular hybrid schemes of the AKP+CW method and present their design equations accordingly.

7.6.1.1 Hybrid 1: 1AKP+3/4CW Method

For this scheme, the AKP method will be applied to link 1 and the CW method applied to links 3 and 4, respectively.

For link 1, following the AKP approach, we have

$$v_1 = r_1^0 \sin\left(\theta_2' - \theta_1^0\right) / \sin\theta_2' \tag{7.40}$$

$$w_1 = l_1^0 - \frac{r_1^0\left(m_2 r_2' \sin\left(\theta_2' - \theta_1^0\right) + m_1 l_2 \sin\theta_1^0\right)}{m_2 r_2' \sin\theta_2'} \tag{7.41}$$

For link 3, by using the CW method from Eq. (7.13), we get

$$\theta_3 = \theta_2 + \pi \tag{7.42}$$

$$m_3 r_3 = l_3 m_2 r_2 / l_2 \tag{7.43}$$

$$m_3{}^* r_3{}^* e^{i\theta_3^*} = m_3 r_3 \mathrm{e}^{i\theta_3} - m_3{}^0 r_3{}^0 \mathrm{e}^{i\theta_3^0} \tag{7.44}$$

For link 4, following the same procedure as for link 3, we can obtain

$$r_3{}' \mathrm{e}^{i\theta_3'} = r_3 \mathrm{e}^{i\theta_3} - l_3 \tag{7.45}$$

$$m_4 r_4 = l_4 m_3 r_3{}' / l_3 \tag{7.46}$$

$$\theta_4 = \theta_3' \tag{7.47}$$

$$m_4{}^* r_4{}^* \mathrm{e}^{i\theta_4^*} = m_4 r_4 \mathrm{e}^{i\theta_4} - m_4{}^0 r_4{}^0 \mathrm{e}^{i\theta_4^0} \tag{7.48}$$

7.6.1.2 Hybrid 2: 1CW+3/4AKP Method

Following the same procedure as mentioned above, we can obtain the design equations.

For link 1,

$$\theta_1 = \theta_2' \tag{7.49}$$

$$m_1 r_1 = l_1 m_2 r_2{}'/l_2 \tag{7.50}$$

$$m_1{}^* r_1{}^* \mathrm{e}^{i\theta_1^*} = m_1 r_1 \mathrm{e}^{i\theta_1} - m_1{}^0 r_1{}^0 \mathrm{e}^{i\theta_1^0} \tag{7.51}$$

For link 3,

$$v_3 = r_3^0 \sin\left(\theta_2 - \theta_3^0\right) / \sin\theta_2 \tag{7.52}$$

$$w_3 = l_3^0 - \frac{r_3^0 \left(m_2 r_2 \sin\left(\theta_2 - \theta_3^0\right) - m_3 l_2 \sin\theta_3^0\right)}{m_2 r_2 \sin\theta_2} \tag{7.53}$$

For link 4,

$$r_3{}' \mathrm{e}^{i\theta_3'} = r_3 \mathrm{e}^{i\theta_3} - l_3 \tag{7.54}$$

$$v_4 = r_4^0 \sin\left(\theta_3' - \theta_4^0\right) / \sin\theta_3' \tag{7.55}$$

$$w_4 = l_4^0 - \frac{r_4^0 \left(m_3 r_3' \sin\left(\theta_3' - \theta_4^0\right) - m_4 l_3 \sin\theta_4^0\right)}{m_3 r_3' \sin\theta_3'} \tag{7.56}$$

7.6.2 Design Examples and Illustrations

We used ADAMS for calculating all joint forces and torques in the motor. We considered three situations for the motors: *situation 1*: both motors are regular constant velocity (CV motor for short) motors; *situation 2*: both motors are servomotors which have a prescribed trajectory; *situation 3*: one motor is a CV motor and the other is a servomotor.

Table 7.4 gives the detailed designed parameters of the parallel robotic mechanism of Fig. 7.4. The second column is associated with the original design, and the

Table 7.4 Parameters of the designed mechanisms

Parameters	Unbalanced	CW	AKP	Hybrid 1	Hybrid 2
l_1 (m)	0.15	0.15	0.13	0.15	0.13
l_2 (m)	0.26	0.26	0.26	0.26	0.26
l_3 (m)	0.26	0.26	0.208	0.208	0.26
l_4 (m)	0.14	0.14	0.0884	0.0884	0.14
l_5 (m)	0.3	0.3	0.3	0.3	0.3
r_1 (m)	0.075	0.0866	0.15	0.0866	0.15
r_2 (m)	0.15	0.15	0.15	0.15	0.15
r_3 (m)	0.08485	0.1	0.12	0.12	0.1
r_4 (m)	0.115	0.141	0.135	0.135	0.141
m_1 (kg)	1	2	1	2	1
m_2 (kg)	2	2	2	2	2
m_3 (kg)	2	3	2	2	3
m_4 (kg)	2	4	2	2	4
I_1 (kg·m^2)	0.01	0.0328	0.01	0.0328	0.01
I_2 (kg·m^2)	0.05	0.05	0.05	0.05	0.05
I_3 (kg·m^2)	0.04	0.0605	0.04	0.04	0.0605
I_4 (kg·m^2)	0.02	0.077	0.02	0.02	0.077
θ_1 (deg)	90	150	150	150	150
θ_2 (deg)	30	30	30	30	30
θ_3 (deg)	225	210	210	210	210
θ_4 (deg)	192.83	188.19	190.89	190.89	188.19

third is the modified design based on CW, and so forth for the remaining columns. For situation 1, we further considered two cases: low speed ($\pi/6$ rad/s) and high speed ($10\pi/3$ rad/s). The results are reported in the following.

7.6.2.1 Results for Situation 1

In all the figures, F_{X1} and F_{X2} represent the X-axis forces (horizontal here) on two motors, respectively; F_{Y1} and F_{Y2} represent the Y-axis forces (vertical) on two motors, respectively, and T_1 and T_2 represent torques on two motors, respectively.

Figures 7.11 and 7.12 show the fluctuation of the driving forces in two directions and the control torques of the parallel robotic mechanism in two motors at a low constant speed of $\pi/6$ rad/s (i.e., the period is 12 s). In Fig. 7.3, the big driving force fluctuations of the unbalanced mechanism are clearly shown. As listed in Table 7.5, the driving force for the unbalanced mechanism rises from the minimum 1.6187 N at time 0.78 s to the maximum 4.957 N at time 8.06 s, followed by a sharp decline to 1.86 N at the end of the period. At this point, a cycle has been completed and a new one begins. Despite far less significant changes, similar trends are seen in all

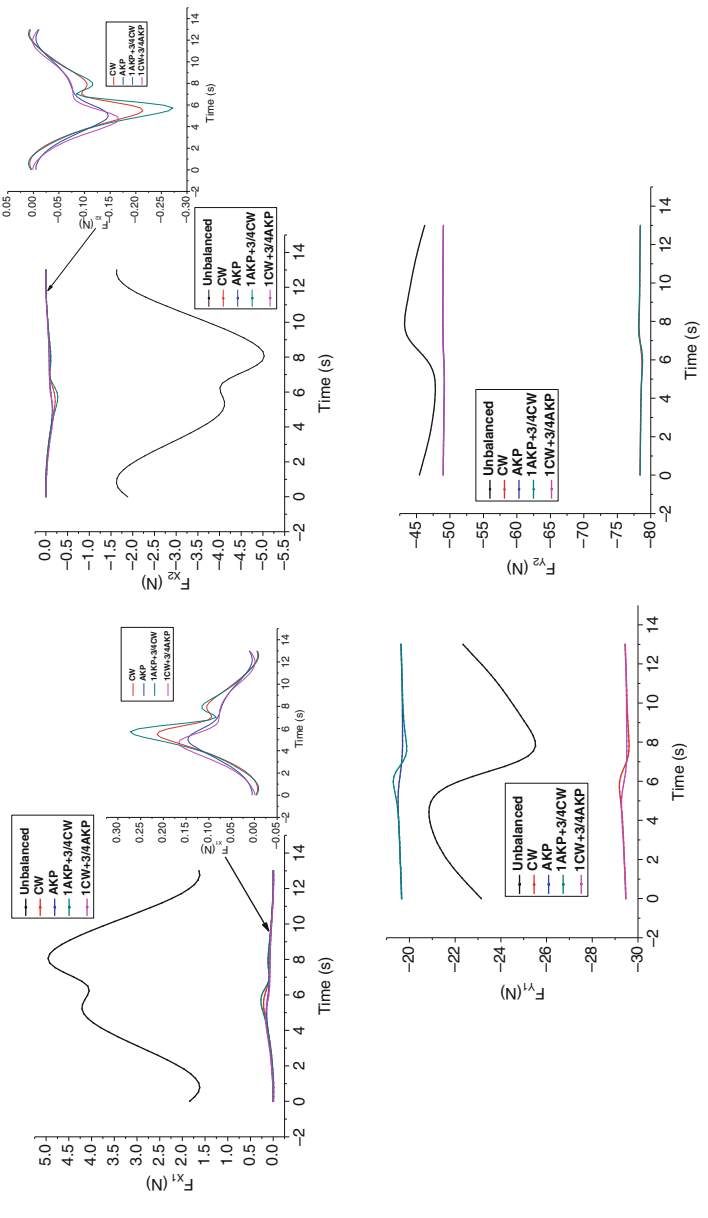

Fig. 7.11 Driving forces for two motors at low speed

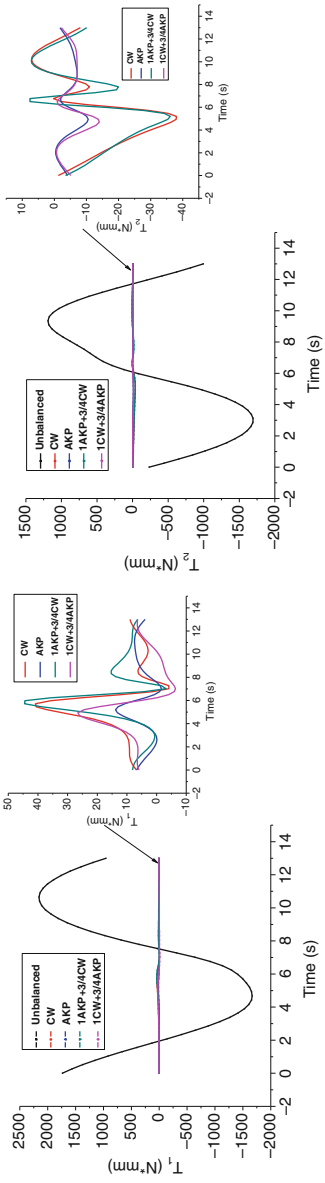

Fig. 7.12 Control torques for two motors at low speed

Table 7.5 Minimum and maximum driving forces of motors at low speed

Force	Range	Unbalanced	CW	AKP	Hybrid 1	Hybrid 2
F_{X1}	Min (N)	1.619	−0.007	0.005	−0.009	−0.001
	Max (N)	4.957	0.214	0.146	0.272	0.167
F_{X2}	Min (N)	−5.030	−0.214	−0.146	−0.272	−0.167
	Max (N)	−1.625	0.007	−0.005	0.009	0.001
F_{Y1}	Min (N)	−25.515	−29.611	−19.699	−19.877	−29.512
	Max (N)	−20.853	−29.186	−19.501	−19.293	−29.275
F_{Y2}	Min (N)	−47.817	−78.687	−49.145	−78.774	−49.178
	Max (N)	−43.219	−78.262	−48.947	−78.190	−48.941

Table 7.6 Minimum and maximum control torques of motors (N mm) at low speed

Force	Range	Unbalanced	CW	AKP	Hybrid 1	Hybrid 2
T_1	Min	−1666.969	−4.135	−1.627	−3.203	−6.373
	Max	2156.143	40.821	13.838	44.473	26.539
T_2	Min	−1693.543	−38.028	−10.568	−36.108	−14.020
	Max	1190.208	7.094	−0.423	7.612	−0.644

the other balanced mechanisms, rising from a minimum to a maximum, followed by a sharp decline at the end of the period. Table 7.5 summarizes the minimum and maximum values of the forces for the unbalanced mechanism and the four balanced mechanisms with different approaches at a low speed.

In general, at low-speed simulation, the unbalanced mechanism fluctuates further more than the balanced mechanisms in terms of force and torque, as shown in Table 7.6. Among the balanced mechanisms, the best performances go to AKP and hybrid 2 (1CW+3/4AKP).

Figures 7.13 and 7.14 describe the fluctuation of the driving forces in the X direction and control torques in two motors at a constant high speed of $10\pi/3$ rad/s. Tables 7.7 and 7.8 list the minimum and maximum driving forces and control torques for two motors, respectively. Comparing Fig. 7.13 with Fig. 7.11, one can see that the distributions of driving forces in the X direction are totally changed when the system operated in a high speed. The differences of the fluctuations of driving forces among all five designs become nonsignificant. The same change trends also appeared for the control torques, as shown in Fig. 7.14 and Table 7.8.

Overall, at high speed, forces and torques considerably differ from those at low speed. The forces nearly increase by 20 times and torques by 100 times. From the simulation results, we can see that the most remarkable phenomenon is that CW and 1AKP+3/4CW are poorer even than the unbalanced mechanism, but still AKP and hybrid 2 (1CW+3/4AKP) are the best.

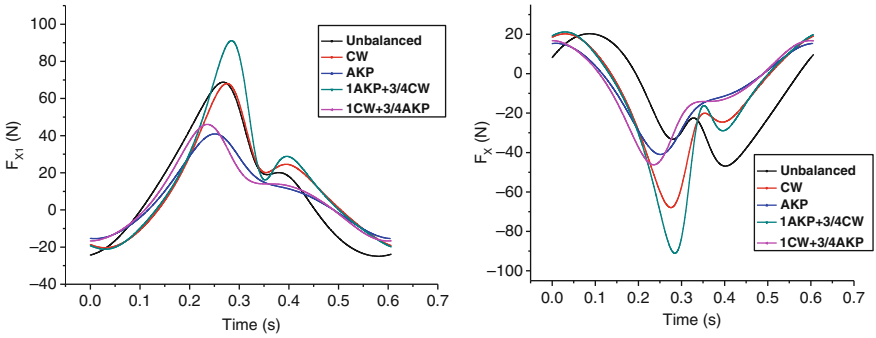

Fig. 7.13 Driving forces for two motors in the *X* direction at high speed

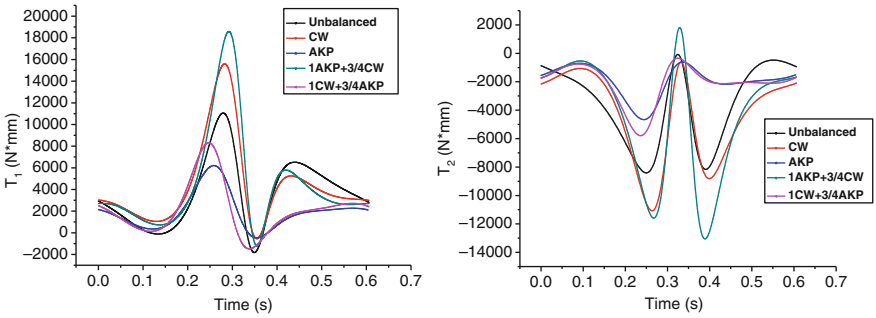

Fig. 7.14 Control torques for two motors at high speed

Table 7.7 Minimum and maximum driving forces of the motors at high speed

Force	Range	Unbalanced	CW	AKP	Hybrid 1	Hybrid 2
F_{X1}	Min (N)	68.803	68.083	40.940	91.156	46.049
	Max (N)	−24.898	−20.328	−15.404	−21.143	−16.676
F_{X2}	Min (N)	−46.863	−67.926	−40.955	−91.127	−46.209
	Max (N)	20.268	20.215	15.400	21.168	16.791
F_{Y1}	Min (N)	−116.555	−102.772	−50.914	−122.878	−62.135
	Max (N)	47.815	66.602	27.916	110.357	28.929
F_{Y2}	Min (N)	−141.116	−174.532	−96.543	−208.603	−107.366
	Max (N)	12.878	−5.260	−17.725	24.701	−16.160

7.6.2.2 Results for Situation 2

For situation 2, the operation duration is 4 s for a full rotation of both motors with varying speeds, and the prescribed trajectories of two motors are defined as follows:

Motor 1:

$$q_{1d} = q_{1d0} + \left(6 \times t^5/4^5 - 15 \times t^4/4^4 + 10 \times t^3/4^3\right) \times 2\pi \quad t \in [0, 4]$$

Table 7.8 Minimum and maximum torques of motors (N mm) at high speed

Force	Range	Unbalanced	CW	AKP	Hybrid 1	Hybrid 2
T_1	Min	−1831.242	−546.258	−472.298	−1215.42	−1485.57
	Max	11066.674	15604.21	6208.644	18605.1	8313.735
T_2	Min	−8406.293	−11073.7	−4660.89	−13051.9	−5791.45
	Max	−71.239	−607.81	−612.595	1807.899	−341.812

Motor 2:

$$q_{2\mathrm{d}} = q_{2\mathrm{d}0} + \left(6 \times t^5/4^5 - 15 \times t^4/4^4 + 10 \times t^3/4^3\right) \times 2\pi \quad t \in [0, 4]$$

Figure 7.15 shows the fluctuation of the driving forces and control torques in two motors. From this figure, it demonstrated that the AKP and hybrid 2 (1CW+3/4AKP) are the best in terms of low driving forces and less fluctuation of the control torques.

7.6.2.3 Results for Situation 3

For situation 3, the operation duration is 4 s and the trajectories of two motors are different and defined as follows:

Motor 1:

$$q_{1\mathrm{d}} = 0.5\pi \times t \quad t \in [0, 4]$$

Motor 2:

$$q_{2\mathrm{d}} = \left(6 \times t^5/4^5 - 15 \times t^4/4^4 + 10 \times t^3/4^3\right) \times 2\pi, \quad t \in [0, 4]$$

Figure 7.16 shows the fluctuation of the driving forces and control torques in two motors under different trajectories, respectively.

Based on these three situations where trajectories are given, AKP and hybrid 2 (1CW+3/4AKP) are the best in terms of less fluctuation of driving forces and less control torques, and the unbalanced mechanism is the worst. However, CW and hybrid 1 (1AKP+3/4CW) appear to be no better than the unbalanced mechanism at high-speed situation.

7.7 Conclusions

The extended AKP method is developed in this chapter. One of the important contributions of this extension lies in the new idea on the adjustment of two pivots on each link. With this design method, the original AKP method was extended to

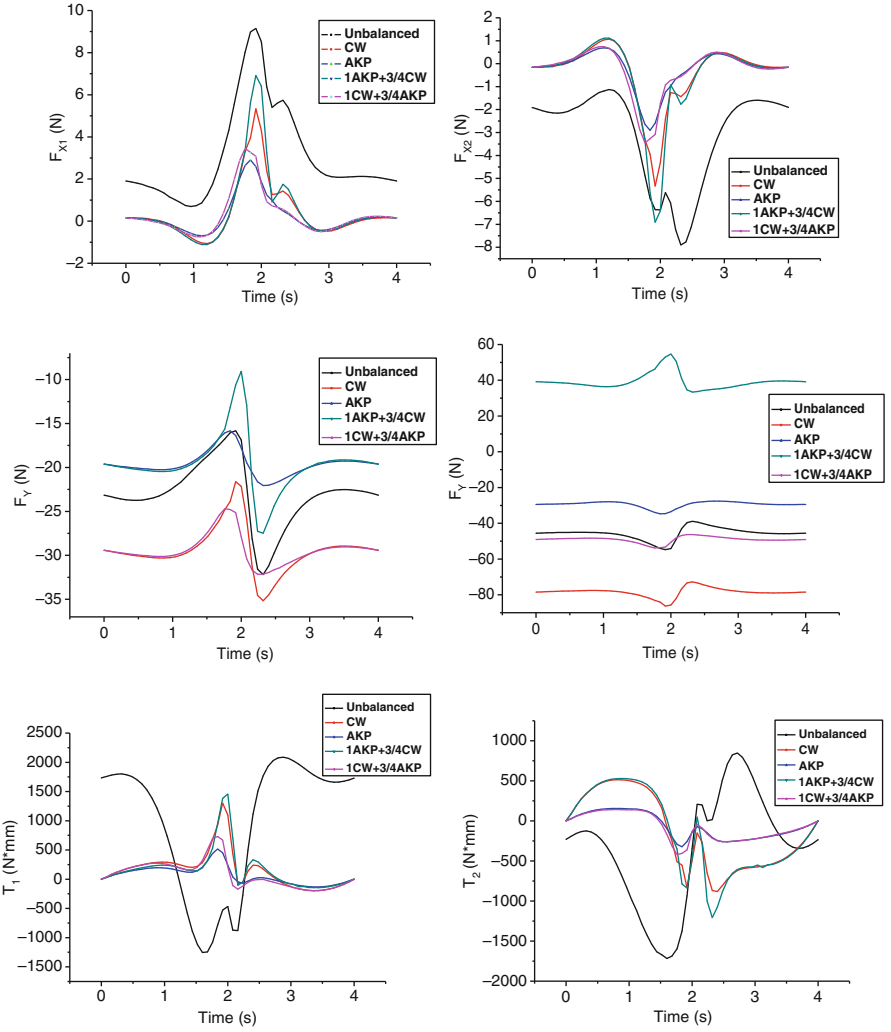

Fig. 7.15 Driving forces and control torques for two motors for the same trajectories

any planar mechanism with "off-line" mass centers. The derived design equations of the extended AKP method are in a general form, from which the special design case with "in-line" mass centers can be readily derived. Two different configurations for three cases: the force unbalanced mechanism, and the force balanced mechanism using the extended AKP method and the CW method, respectively, are studied to demonstrate the effectiveness of the extended AKP method. The joint forces of the individual pivots are calculated at both low speeds and high speeds for these

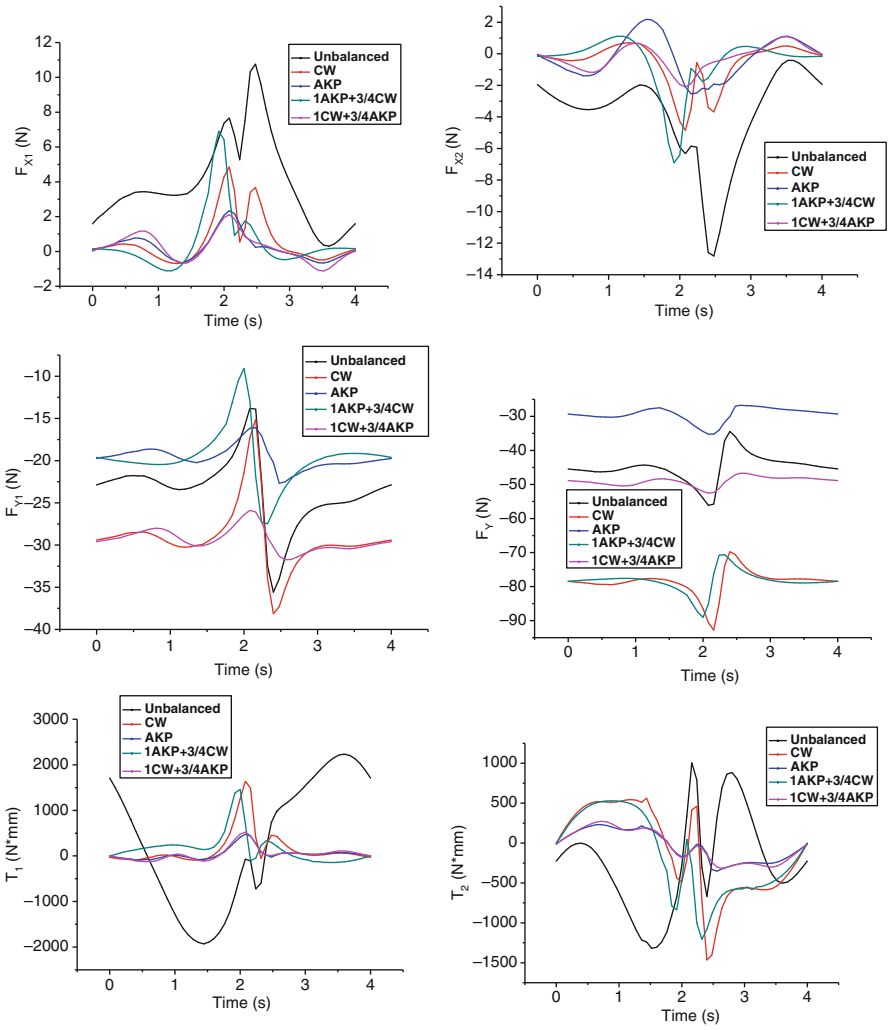

Fig. 7.16 Driving forces and control torques for two motors for different trajectories

configurations. All the results have shown that the extended AKP method is better than the CW method in terms of the joint force reductions and the variation decrease at high speeds.

It should be noticed that the static balancing solution has some demerit when the mechanism runs at high speeds. In this case, the inertia forces becomes the dominant term in the dynamics. Since the CW method adopts the adding mass approach for force balancing purpose, its inertia force takes more weight. While with the extended AKP method, the total mass of the system is unchanged; therefore the inertia force does not differ significantly from the unbalanced mechanism.

In addition, following the hybridization principle, the hybrid AKP+CW method was proposed for the force balancing. Two different hybrid schemes are designed for the parallel robotic mechanism and their performances are compared with AKP, CW, and unbalanced mechanism. Simulation results show that AKP and hybrid 2 (1CW+3/4AKP) can achieve good performance in all situations. As the operating speed increases, CW and hybrid 1 (1AKP+3/4CW) get worse. When the operating speed goes up to $10\pi/3$ s^{-1}, CW and hybrid 1 (1AKP+3/4CW) are even worse than the unbalanced mechanism.

It should be noted that, in the force balancing with the CW+AKP approach, certain parameters need to be selected. In this study, the optimal selection of these parameters has not been considered. The optimal selection of design parameters in the CW+AKP approach will be addressed in future. Another work is planned in the future on moment balancing and torque balancing with this hybrid approach.

References

1. Wang, J.G., Gosselin, C.M.: Static balancing of spatial four-degree-of-freedom parallel mechanisms. Mech. Mach. Theory **35**(4), 563–592 (2000)
2. Wang, Z.H.: Mechatronic design to real-time controllable mechanical systems: force balancing and trajectory tracking. M.Sc. thesis, University of Saskatchewan (2000)
3. Xi, F.F., Sinatra, R.: Effect of dynamic balancing on four-bar linkage vibrations". Mech. Mach. Theory **32**(6), 715–728 (1997)
4. Berkof, R.S., Lowen, G.G.: A new method for completely force balancing simple linkages". Trans. ASME J. Eng. Ind. **91**(B), 21–26 (1969)
5. Bagci, C.: Shaking force balancing of planar linkages with force transmission irregularities using balancing idler loops. Mech. Mach. Theory **14**(4), 267–284 (1979)
6. Gosselin, C.M.: Static balancing of spherical 3-DoF parallel mechanisms and manipulators". Int. J. Rob. Res. **18**(8), 819–829 (1999)
7. Ouyang, P.R., Zhang, W.J., Wu, F.X.: Nonlinear PD control for trajectory tracking with consideration of the design for control methodology. IEEE IRAC **4**, 4126–4131 (2002)
8. Ouyang, P.R.: Force balancing design and trajectory tracking control of real-time controllable mechanisms. M.Sc. thesis, University of Saskatchewan (2002)
9. Ouyang, P.R., Zhang, W.J.: Force balancing of robotic mechanisms based on adjustment of kinematic parameters. ASME J. Mech. Des. **127**(3), 433–440 (2005)
10. Zhang W.J., Ouyang, P.R., Gupta, M.M., Sun, Z.H.: A novel hybridization design principle for intelligent mechatronics systems. ICAM 2010, Japan (2010)
11. Huang, J., Ouyang, P.R., Cheng, L., Zhang, W.J.: A Hybrid Approach To Force Balancing Of Robotic Mechanisms. Proceedings of the ASME 2010 International Mechanical Engineering Congress & Exposition (IMECE 2010), pp. 735–744 (2010)